HONOURS III PROJECT

Modelling Populations with a Case Study on Orange Roughy in New Zealand

Damian Campbell
Department of Mathematics and Statistics
University of Canterbury

2005

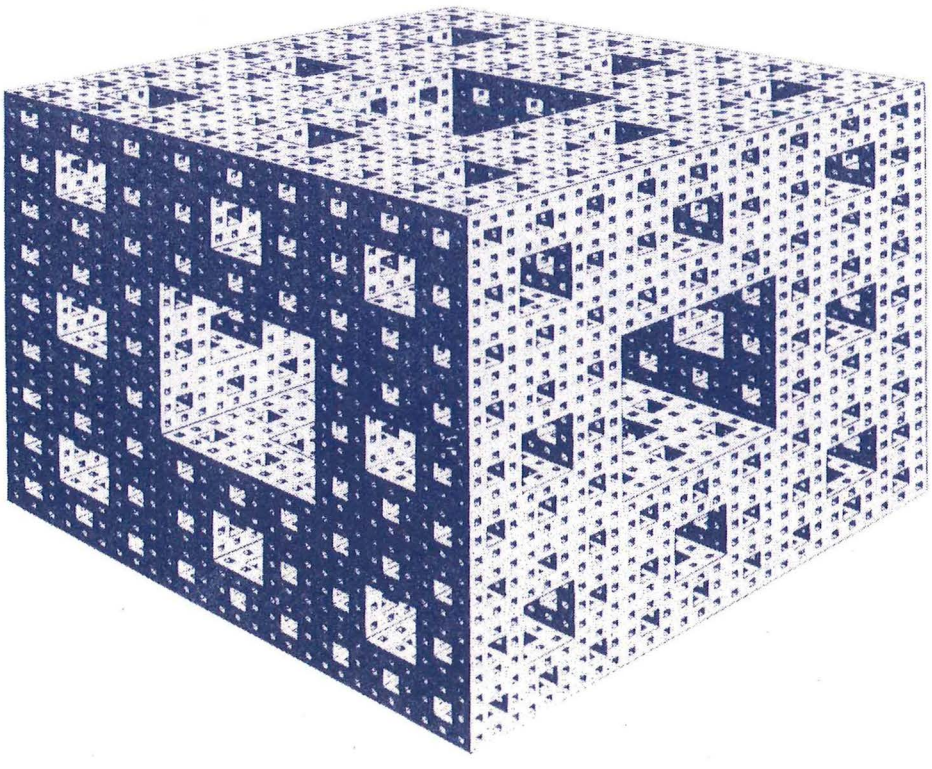

Modelling populations with a case study on orange roughy in New Zealand

Damian Campbell

2005

Contents

0.1 Introduction

The dynamics of mathematical models used for modelling populations will be investigated. Mathematical models have many applications, these will be mentioned throughout the paper. Mathematical models are particularly useful for modelling fish populations. Most fish populations are not farmed, and fish are taken from their wild environment. Models must be used to monitor population levels, and to determine the affect of harvesting.

The use of simplifications is common, as models that could more accurately model a biological system are very hard to solve and require many parameters that must be measured. For example a food web that exists in nature could potentially have 50 or more species, each with a complex life cycle and each having an equally complex interaction with other species in the food web. Food webs investigated will have at most three species, so analytic solutions can be found and to reduce the number of parameters. These species will usually be prey, predator and superpredator, but alternatively can be thought of as plant, herbivore and predator. This is the beauty of using mathematical modelling, predator-prey dynamics are analysed exactly the same way as herbivore-plant dynamics, even though biologically they are different. Different topologies of food webs will be examined to determine the affect of the topology on population dynamics.

A single species can be modelled with age structure in its population, by using a partial differential equation. The model examined negates interactions between species, but allows a single species to be modelled in more detail. The partial differential equation model is approximated using an individual based model, where each individual in the population ages at a constant rate, and reproduction and mortality will not be deterministic. Both of these will occur as poisson processes.

The individual based model developed is used to model the population of orange roughy in New Zealand waters. Parameters concerning recruitment and mortality of orange roughy are examined. The sensitivity of these parameters are investigated, as many published parameters are best estimates or educated guesses. Orange roughy has suffered severe losses due to fishing, the estimate of current biomass is just 20% of virgin biomass. The population response to different harvesting rates is examined in detail, in particular to find if there is a sustainable harvest rate, given the population is currently so low.

1 Deterministic Food Web Models with two species

The building blocks of a general two species food web model with prey x and predator y have the form:

$$\begin{aligned} \frac{dx(t)}{dt} &= \dot{x} = xf(x,y), \\ \frac{dy(t)}{dt} &= \dot{y} = yg(x,y), \end{aligned} \tag{1}$$

where f and g are functions, governing both growth and death of x and y respectively. Equation (1) has the form $xf(x,y)$ since growth and death of x depend on x, so a common factor of x has been taken out. Similarly $yg(x,y)$ is used. This chapter will focus on different choices of f and g, and the advantages of each choice.

1.1 Lotka-Volterra Systems

The most simple food webs are the Lotka - Volterra equations, derived in 1926 by Lotka and independently by Volterra in 1927 (Murray [1]). As in May [4] and Murray [1], the Lotka-Volterra equations have $f(x,y) = a - by$ and $g(x,y) = cx - d$, such that system (1) becomes:

$$\begin{aligned} \dot{x} &= ax - bxy, \\ \dot{y} &= cxy - dy. \end{aligned} \tag{2}$$

These equations with $a, b, c, d > 0$, is interpreted as showing the prey x grows exponentially at rate a (also called Malthusian growth) in the absence of predators y. Growth of the prey population is limited only by predation which occurs at rate b, and is dependent on the population densities of predator and prey. Predators die at rate d, and c is a measure of the efficiency of predators to convert prey caught into growth (May [4]).

Solving $\dot{x} = 0$ and $\dot{y} = 0$ in system (2) gives two fixed points (0,0) and $(\frac{d}{c}, \frac{a}{b})$. By looking at the linearised system of the system (2) at the trivial fixed point (0,0), it is clear it is a saddle point for all $a, d > 0$ (see appendix A for details). Similarly, the fixed point $(\frac{d}{c}, \frac{a}{b})$ is a centre for all $a, d > 0$ (see appendix A). Figure 1 illustrates a typical phase portrait of the system with parameter values $a = 1, b = 2, c = 1, d = 1$. The figure shows ellipses centred at $(\frac{d}{c}, \frac{a}{b})$ $(= (1, \frac{1}{2}))$ and a saddle at (0,0), agreeing with the result predicted. A time series of the

populations would show that both populations oscillate periodically forever.

Murray [1] shows that data over the period 1875-1904 for lynxes and hares in Canada, almost have an elliptical orbit in the phase plane. However this orbit is oriented clockwise in contrast to figure 1 in which orbits are oriented anticlockwise, implying that hares eat lynxes (Gilpin [3]). So the model described by system (2), has limitations for modelling populations, and more realistic models must be derived.

Lotka-Volterra systems as in system (2) are conservative systems i.e. there is some quantity in the system that is conserved, and all fixed points are centres or saddles. The conserved quantity for system (2) is (see appendix A):

$$V(x,y) = a\log(y) + d\log(x) - cx - by.$$

This conserved quantity has no intuitive biological interpretation. This conservative quantity arises because the simplicity of the functions $f(x,y) = f(y) = a - by$ and $g(x,y) = g(y) = cx - d$, makes $\frac{dy}{dx}$ separable. Most systems are not conservative.

1.2 Logistic prey growth functions

In system (2) it is assumed that the prey grows exponentially in the absence of predators. This assumption is not realistic for most food webs, where there is a finite amount of resources available for consumption. A more realistic model incorporates a 'cap' on the growth of the prey (May [4]). The logistic equation for growth of a single prey species x:

$$\dot{x} = rx\left(1 - \frac{x}{K}\right), \tag{3}$$

provides this information (May [4]). The logistic growth model states the population grows at a rate proportional to some positive constant, r, for low population levels, but as the population increases to near the carrying capacity, K, population growth slows. The carrying capacity is the total number of prey the environment is able to support due to resource limitations. Trivially K is positive since a negative population has no meaning. In equation (3), K is a globally attracting fixed point for all $x > 0$, and $x = 0$ is globally repelling. In Waltman [7], equation (3) is shown to accurately model population growth of E. coli bacteria.

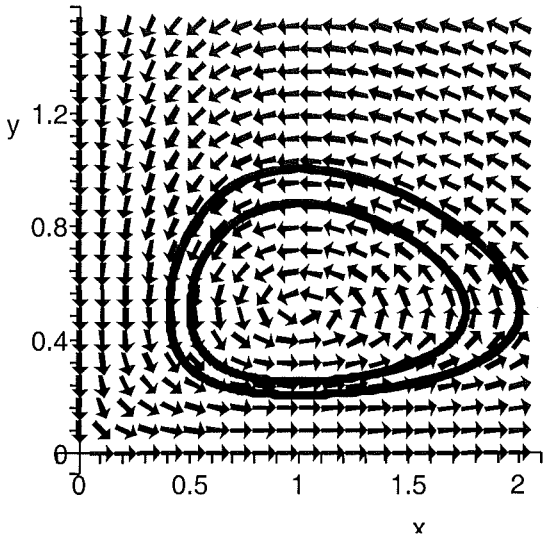

Figure 1: Phase portrait for the Lotka-Volterra system, given in system (2) showing prey (x) populations against predator (y) populations. Two periodic orbits for the different initial conditions (1,1) and (0.5,0.5) are shown. Parameter values are $a = c = d = 1$ and $b = 2$.

Equation (3) is by no means a unique function for prey growth, May [4] gives a delay differential equation:

$$\dot{x} = rx\left(1 - \frac{x(t-T)}{K}\right), \tag{4}$$

that also models prey population growth. In this model T is the lag of the species to respond to limited resource availability, and r and K are the same as in equation (3). Equation (4) has a stable fixed point for $rT < \frac{1}{2}\pi$ and a stable limit cycle for $rT > \frac{1}{2}\pi$ (May [4]). The added feature of limit cycles in eqn (4) can make it suitable for modelling a single non-interacting species, in May [4] it accurately models the oscillating population of a blowfly species. De Feo and Rinaldi [9] show a two species food web with logistic prey growth as given in equation (3), exhibits limit cycles. Thus eqn (4) will not be used in any food web models, as it adds an additional parameter - T and offers no extra information when used in a two species food web.

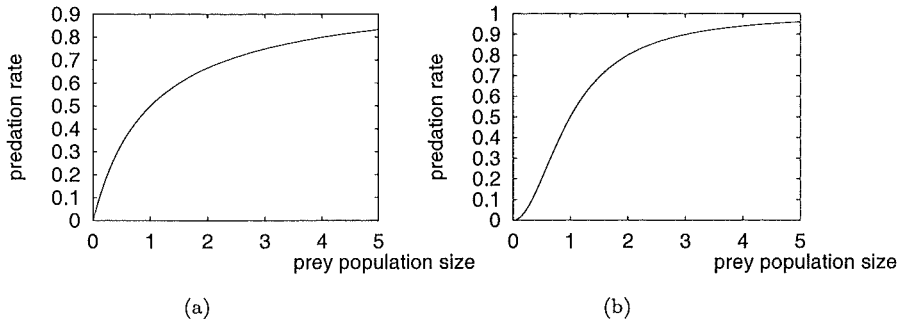

(a) (b)

Figure 2: Plots of two different types of predation functions, $h(x)$. Plots show predation rate against the prey population size. (a) A Holling type II function $h(x) = \frac{x}{x+1}$, the predation rate is linear for low populations, but the predation rate is capped for high populations. (b) A Holling type III function $h(x) = \frac{x^2}{x^2+1}$, the predation rate is not linear for low populations, and the predation rate is capped due to predator saturation. In both (a) and (b) the predation rate is half the maximum rate when the population size is 1.

The food web given in system (2) with logistic prey growth becomes:

$$\begin{aligned} \dot{x} &= rx\left(1 - \frac{x}{K}\right) - bxy, \\ \dot{y} &= cxy - dy. \end{aligned} \tag{5}$$

In system (5) the growth rate of the prey is r, K is the carrying capacity as defined for equation (3). The inclusion of the logistic prey growth function in system (5), means it is not a conservative system. All systems mentioned from now on are not conservative.

1.3 Predation functions

The predation rate in system (5) is constant at rate b, for all prey population sizes. The term bxy in system (5) means prey is caught at rate b whenever there is a predator-prey encounter. The food web described by system (5) can be extended by replacing bxy with $h(x)y$, where $h(x)$ is a predation function that varies for different prey population sizes.

Figures 2a and b are predation functions that will be used to make more realistic food web models. Both the Holling type II function $h(x) = \frac{Ax}{x+B}$ in figure 2a and the Holling type III function $h(x) = \frac{Ax^2}{x^2+B}$ in figure 2b have a maximum

predation rate, because for high prey populations, predators become saturated and are unable to catch any more prey. For both functions the maximum predation rate is A, and B is the prey population size at which the predation rate is equal to half the maximum rate i.e. $\frac{A}{2}$ (De Feo and Rinaldi [9]). The effect on food web dynamics of including these non-linear predation functions will be examined.

First a food web with Holling type II predation function will be examined. Incorporating a Holling type II function in system (5) gives:

$$\begin{aligned} \dot{x} &= rx\left(1-\frac{x}{K}\right) - A\frac{xy}{x+B}, \\ \dot{y} &= c\frac{xy}{x+B} - dy. \end{aligned} \tag{6}$$

The inclusion of a Holling type II function in system (6), means predator growth is limited because of the maximum predation rate. De Feo and Rinaldi [9] show system (6) has a stable fixed point for $\frac{Bd}{cA-d} < K \leq \frac{Bd+ABc}{cA-d}$ or a stable limit cycle for $K > \frac{Bd+ABc}{cA-d}$. To reduce the number of parameters, analysis of system (6) will be done by reducing it to a non-dimensional form. The non-dimensionalised system is (see appendix B for details):

$$\begin{aligned} \dot{N} &= N\left(1-\frac{N}{\rho}\right) - \frac{NP}{N+1}, \\ \dot{P} &= \beta\left(\frac{N}{N+1} - \alpha\right)P. \end{aligned} \tag{7}$$

N is the dimensionless prey, P is the dimensionless predator and ρ, β and α are dimensionless parameters, see appendix B for forms of these dimensionless variables and parameters. Fixed points of this system are (0,0), (ρ,0) and $\left(-\frac{\alpha}{\alpha-1}, -\frac{\alpha+\alpha\rho-\rho}{\rho(1-2\alpha+\alpha^2)}\right)$, the third fixed point is the most important as it shows coexistence of the two populations. The coexistent populations are stationary for $\rho < \frac{1+\alpha}{1-\alpha}$, but oscillate for $\rho > \frac{1+\alpha}{1-\alpha}$ (see appendix C). Figure 3 is a schematic bifurcation diagram for system (7) with parameter values $\alpha = \frac{3}{4}$ and $\beta = \frac{1}{2}$, while ρ varies to show changes in stability. Figure 3 shows for ρ between 0 and 3 the fixed point (ρ,0) is stable (shown by solid line), so only the prey survives, because the carrying capacity is too small to support a predator. This fixed point then changes stability, and the coexistent fixed point $\left(-\frac{\alpha}{\alpha-1}, -\frac{\alpha+\alpha\rho-\rho}{\rho(1-2\alpha+\alpha^2)}\right)$ becomes stable. For ρ between 3 and 7 the coexistent populations are stationary since the fixed point is stable. For values of ρ larger than 7 this fixed point

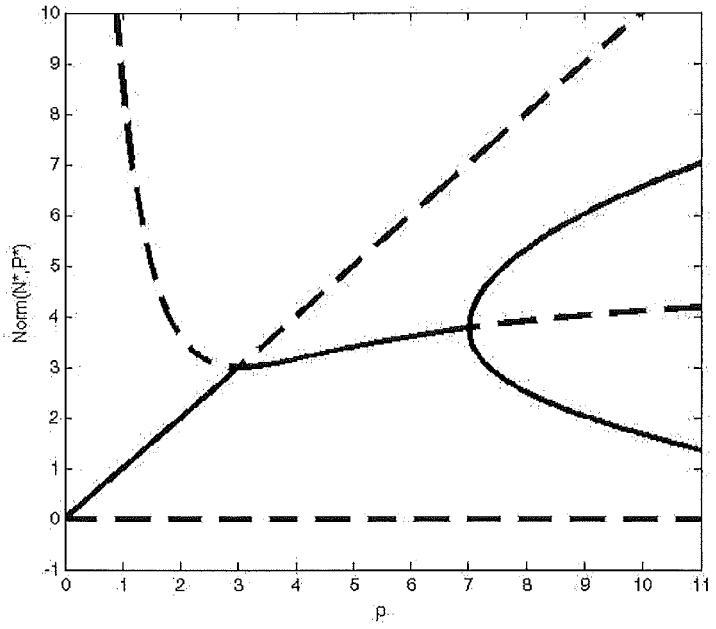

Figure 3: Schematic bifurcation diagram for system (7), showing the 2-norm of the fixed point (N^*, P^*) against parameter ρ. Solid lines show a stable fixed point and dashed lines show unstable fixed points. For $\rho > 7$ a limit cycle appears. Other parameter values in system (7) are $\alpha = \frac{3}{4}$ and $\beta = \frac{1}{2}$

becomes unstable (shown by a dashed line), and a stable limit cycle appears: the predator and prey still coexist but their populations are now cyclic. The fixed point (0,0) is unstable for all positive values of ρ.

1.4 Excitability in a two species food web

Including a Holling type III function: $h(x) = \frac{Ax^2}{x^2+B^2}$ gives significantly different dynamics to a food web with Holling type II functions. Holling type III functions are not linear for low values of x, for low prey populations the predation rate is significantly lower as shown in figure 2b. This is realistic because for low prey populations predators will struggle to find prey and hence the predation rate will be lower. The big addition that Holling type III functions give is that as in Truscott and Brindley [6] a food web model with Holling type

III predation function can exhibit excitable states. An excitable state occurs when a small perturbation from the initial condition leads to a significantly higher population level before returning to the steady state. A system with Holling type II functions cannot exhibit excitability. Excitability is shown in [6] to be applicable to phytoplankton, zooplankton systems in which blooms occur.

Incorporating a Holling type III predation function in a food web model gives (Truscott and Brindley [6]):

$$\begin{aligned} \dot{x} &= rx\left(1-\frac{x}{K}\right) - A\frac{x^2y}{B^2+x^2}, \\ \dot{y} &= c\frac{x^2y}{B^2+x^2} - dy. \end{aligned} \tag{8}$$

This system has one stable fixed point for which there is coexistence of x and y.

Figures 4a and b show populations of x and y for system (8) with different initial conditions, and parameter values $r = 0.3$, $K = 108$, $A = 0.7$, $B = 5.7$, $d = 0.012$ and $c = 0.05$ (Truscott and Brindley [6]). In figure 4a the populations of x (solid line) and y (dotted line) increase then return to steady state quickly. Figure 4b shows a small perturbation of 0.01 from the initial conditions causes a big increase in prey population before returning to the steady state some time later. This is a bloom in the prey population, and is found in excitable systems. The predator population also increases slightly in figure 4b, but not as significantly as the prey population.

1.5 Mutualisms and competition

Mutualisms between two species occur when both species benefit from the relationship (Campbell et.al. [11]). This differs from predator-prey models that have been studied in the early part of this paper, in which the relationship is only beneficial to the predator. An example of a mutualism is Rhizobium nitrogen-fixing bacteria living in the roots of legume plants, in which both plant and bacteria benefit. The bacteria gets shelter and the plant gets nitrogen from the bacteria which is important for protein (Campbell et. al. [11]). A mathematical model of a mutualism for which both species have logistic growth is (Murray

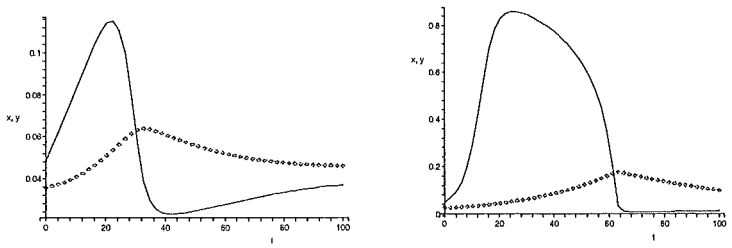

(a) (b)

Figure 4: System (8) exhibiting excitable behaviour with parameter values from [6] $r = 0.3, K = 108, A = 0.7, B = 5.7, d = 0.012$ and c=0.05. Figures show populations of prey x (solid line) and predator y (dotted line) over time. (a) For initial conditions (0.048,0.036), prey population increases slightly before returning to steady state. (b) A small perturbation in initial conditions to (0.048,0.026), causes a big increase in prey population (note different scale on vertical axis) before finally returning to the steady state.

[1]):

$$\dot{x} = a\,x\left(1 - \frac{x}{K_1}\right) + bxy \tag{9}$$
$$\dot{y} = c\,y\left(1 - \frac{y}{K_2}\right) + dxy$$

In system (9) a and c are positive growth rates of x and y respectively and b is a measure of the positive contribution of species y to the growth of x. Similarly d measures the positive effect of species x on the growth of y. K_1 and K_2 are the carrying capacities for species x and y respectively. In system (9) populations of x and y are only limited by their carrying capacities, population size is no longer limited by the presence of the other species. Due to the logistic growth functions, system (9) has a stable fixed point for coexistence of x and y: $\left(\frac{cK_1(a+bK_2)}{ca-bdK_1K_2}, \frac{aK_2(c+dK_1)}{ca-bdK_1K_2}\right)$. If b and d are both zero, i.e. neither species benefits the other, then this fixed point reduces to (K_1, K_2), i.e. both species populations will be at the carrying capacity of the environment. But in a mutualism both species benefit from the others presence so b and d are positive. This means the coexistent populations of x and y are greater than K_1 and K_2 respectively. So mutualisms allow populations to be larger than the carrying capacity of the environment. If Malthusian growth of both species was used in system (9) then

both x and y would grow unbounded, and there would be no stable fixed point for coexistence.

If two species both rely on the same resource, e.g. food or shelter, for survival, but neither preys on the other, the two species are in competition. An example of interspecific competition is bellbirds and wasps competing for honeydew secreted by scale insects from native New Zealand beech trees (Murphy and Kelly [12]). A model for interspecific competition from Boyce and Diprima [5] is:

$$\begin{aligned} \dot{x} &= a\,x\left(1-\frac{x}{K_1}\right) - bxy \\ \dot{y} &= c\,y\left(1-\frac{y}{K_2}\right) - dxy \end{aligned} \tag{10}$$

a, c, K_1 and K_2 are parameters with the same definition as for system (9). In system (10) b and d measure the negative effect of one species on the other. The population of each species is now restricted by the presence of the other species as well as the carrying capacity of the environment. System (10) could have been defined as system (9) but with b and d negative. This is because competition occurs when two species have a negative effect on one another while mutualism occurs when the effects are positive.

The model described by system (10) leads to either x or y surviving, because the fixed points $(K_1, 0)$ and $(0, K_2)$ are stable. The fixed point with both x and y present $\left(\frac{cK_1(a-bK_2)}{ca-bdK_1K_2}, \frac{aK_2(c-dK_1)}{ca-bdK_1K_2}\right)$ is unstable. The initial conditions determine which species will survive. This means that competitive coexistence i.e. existence of both x and y, is excluded by this model. This is a very important aspect of population biology, so a more realistic model that incorporates this behaviour must be developed. Competition will be examined in more detail in chapter 2 with a three species food web, as this allows coexistence.

1.6 Food web models not studied

There are many deterministic food web models that have not been investigated. For example, chemostat models, which are concerned with growth of bacteria fed at a constant rate in a reactor.

A non-dimensionalised model for two competing species of bacteria feeding

on a resource supplied to the system at a constant rate is (Waltman [7]):

$$\begin{aligned}
\dot{S} &= 1 - S - \frac{m_1\, x\, S}{a_1 + S} - \frac{m_2\, y\, S}{a_2 + S}, \\
\dot{x} &= \frac{m_1\, x\, S}{a_1 + S} - x, \\
\dot{y} &= \frac{m_2\, y\, S}{a_2 + S} - y,
\end{aligned}$$

where S is the resource, and x and y are competing species of bacteria. Since chemostat models are only useful for modelling species being fed at a constant rate they have little relevance to populations that occur in nature. Thus no further analysis of them will be done.

Models for competing stage structured populations are also used as deterministic population models but are not investigated. Populations can also be modelled using discrete models.

2 Extending food web models

Food web models can easily be extended to study more than two species. Models with three species can incorporate greater complexity, and species can exhibit different types of foraging and competition behaviour than in models introduced earlier. Different topologies for three species food web models studied in this chapter are shown in figure 5. In this figure an arrow between two species indicates the species at the start of an arrow preys on the species at the other end.

Figure 5a shows a food chain in which predation only occurs on species one trophic level lower, figure 5b is the topology of two predators y and z competing for the same prey x, but neither predates on the other. Figure 5c depicts an adaptable superpredator z that can choose to predate on species x or y. In this topology z and y are competitors as well as z preying on y.

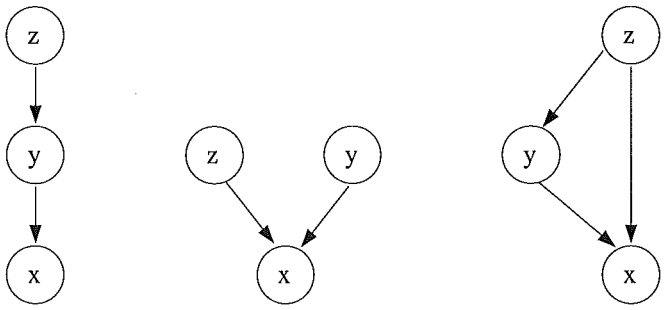

Figure 5: Different food web topologies for 3 species x,y and z used in this paper. An arrow between two species means the species at the start of the line predates the species at the other end. a) is a food chain in which all species predate only on species in one trophic level lower, b) is competing species, in which y and z are competing for x. In c) the adaptable superpredator z predates on both x and y.

2.1 Three Species Food Chain

A food chain is a simple idea, every species in the model preys on the species in a trophic level one lower than its own. A model to describe this interaction is found by extending a two species predator-prey model to include a superpredator

in the trophic level one higher than the predator.

Extending system (6) to include a superpredator z that preys on y with Holling type II predation response function gives (De Feo and Rinaldi [9]):

$$\begin{aligned} \dot{x} &= rx\left(1-\frac{x}{K}\right) - b\frac{xy}{x+B}, \\ \dot{y} &= cb\frac{xy}{x+B} - e\frac{yz}{y+C} - d_1 y, \\ \dot{z} &= f\frac{yz}{z+C} - d_2 z, \end{aligned} \tag{11}$$

where r,K,c,b and B all have same meaning as in the two species system (6). d_1 and d_2 are the death rates of y and z, e is the maximum predation rate of z on y, f is the efficiency of the superpredator and C is the population size of y for which the predation rate of z is half the maximum. System (11) is often called a Rosenzweig-Macarthur tritrophic food chain model (De Feo and Rinaldi [9]).

Bifurcations that occur in system (11) with changes in K has applications to nutrient supply to ecosystems. This can determine the affect on food web dynamics of adding or removing nutrient, since K is the amount of nutrient in the system.

Hastings and Powell [10] first showed the Rosenzweig-Macarthur tritrophic food chain exhibits chaos. A two species food web as in chapter 1 only ever has a stable fixed point or a stable limit cycle. This shows the extra complexity a three species food web model can exhibit. De Feo and Rinaldi [9] show system (11) has a stable fixed point with only x and y present, or coexistence of x,y and z in many different states such as a stationary fixed point, low frequency limit cycle, high frequency limit cycle or chaos, depending on parameter values. If the system is nutrient rich i.e. K is high, then all three species coexist in a high frequency limit cycle state, or the superpredator becomes extinct. If the system is undersupplied in nutrient, i.e. K is small, then coexistence of all three species occurs as chaos, low frequency limit cycles or stationary coexistence (De Feo and Rinaldi [9]). So increasing nutrient in a stable system may not increase biomass in the system and can even lead to extinction of the superpredator. This also shows that undersupplied and oversupplied systems can exhibit similar dynamics, for example chaos and high frequency limit cycles are very similar, yet chaos is typical of a nutrient deficient system and high frequency limit cycles occur for nutrient rich systems.

2.2 Competition for a common resource

In chapter 1 interspecific competition was looked at for two species in competition. The two species model gives the result that coexistence of two competitors is not possible. The inclusion of a third species makes coexistence possible. The system governing this interaction has only one prey species, but two species that prey on it, for simplicity the two competitors do not predate one another. Therefore the only effect that they have on each other is they consume the prey the other is after. Hsu, Hubbel and Waltman [8] give a model describing two competing species, where as in system (11), prey grow logistically and all predation functions are Holling type II:

$$\begin{aligned}
\dot{x} &= rx\left(1-\frac{x}{K}\right) - b\frac{xy}{\gamma_1\,(x+B)} - c\frac{xz}{\gamma_2\,(z+C)},\\
\dot{y} &= b\frac{xy}{x+B} - d_1 y,\\
\dot{z} &= c\frac{xz}{x+C} - d_2 z.
\end{aligned} \tag{12}$$

γ_1 and γ_2 are efficiency rates of y and z respectively to convert prey caught into growth. Although this form may appear different, γ_1 and γ_2 have exactly the same effect as the efficiency factors c and f in system (11).

A minimum requirement for coexistence of y and z in system (12) is that the parameter values satisfy (Hsu, Hubbel and Waltman [8]):

$$\frac{b-d_1}{c-d_2} < \frac{d_1}{d_2} < \frac{C(b-d_1)}{B(c-d_2)} \tag{13}$$

$$\text{and} \qquad K > \frac{Cbd_2 - Bcd_1}{cd_1 - bd_2}. \tag{14}$$

There is parameter values that satisfy the above conditions, but do not result in coexistence of y and z. However all parameter values that allow coexistence of y and z do satisfy the above conditions.

Figure 6 shows that coexistence of predators occurs and that all species have cyclic populations. The population of prey grows rapidly from initial condition $x(0) = 1$ to carrying capacity $K = 1000$ then decreases rapidly due to increase in predator populations, and begins to oscillate only after predator z starts oscillating. All populations continue to oscillate over time. Numerical experiments in [8] show that populations of competing predators are always cyclic. There is no analytic proof of this cyclic behaviour.

Conditions (13) and (14) give parameter values for which one predator will

survive and the other becomes extinct. If K is small and does not satisfy condition (14), only the predator most well suited to fast growth and small populations will survive, this predator is referred to as "r selected" (Hsu, Hubbel and Waltman [8]). Similarly if K is large, even if condition (14) is satisfied, only the "K selected" predator will survive, that is the predator most suited to slow growth and large populations. This illustrates the ecological niche of the predators, only the predator most suited to the ecological niche will survive.

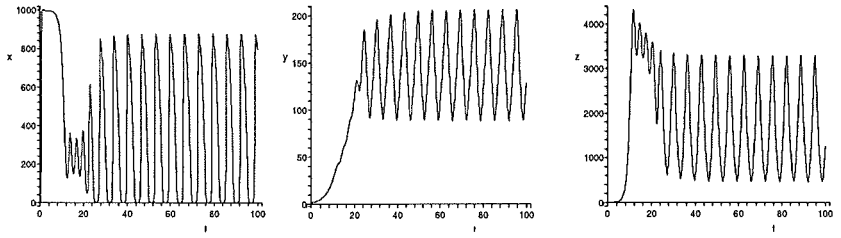

(a) Population of prey x (b) Population of predator y (c) Population of predator z

Figure 6: Cyclic coexistence of populations of prey and competing predators in system (12) over time. Parameter values are: $B = 100$, $C = 720$, $r = 20log(2)$, $d1 = \frac{log(2)}{2}$, $d2 = log(2)$, $\gamma_1 = 0.1$, $\gamma_2 = 1.14$, $b = log(2)$, $c = 4log(2)$ and $K = 1000$, initial conditions $x(0) = 1$, $y(0) = 2$, $z(0) = \frac{1}{2}$ ([8]).

For example with parameter values given in figure 6, except K=400, K now violates condition (14), so coexistence is not possible. Predator y survives since it is a more efficient predator than x, because $(\frac{1}{\gamma_1} > \frac{1}{\gamma_2})$, and predates at a higher rate for lower prey densities because $B < C$. Figures 7a and b show that for K=400, only species x and y survive, while figure 7c shows predator z becomes extinct. The populations of x and y still oscillate in the absence of z. This means the predator y is an "r selected" predator.

2.3 Adaptable predation

Models described earlier deal with predators and superpredators that predate exclusively on one species. But a superpredator can forage on the prey when prey populations are high, and switch to foraging on the predator when prey populations are small. This is often what happens since a constant source of food from one particular species is unlikely. A model incorporating this information

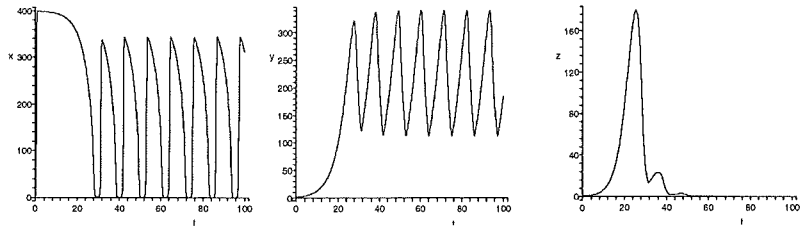

(a) Population of prey x (b) Population of predator y (c) Population of predator z

Figure 7: For low carrying capacity (K) only the "r selected" predator survives. In this case y survives and z becomes extinct. All parameter values are the same as for figure 6 except now $K = 400$.

is (Křivan [13]):

$$\begin{aligned}
\dot{x} &= rx\left(1 - \frac{x}{K}\right) - b\frac{xy}{x+B} - e_1\frac{xz}{x+E_1} \\
\dot{y} &= cb\frac{xy}{x+B} - e_2\frac{yz}{y+E_2} - d_1 y \\
\dot{z} &= f\left(e_1\frac{xz}{x+E_1} + e_2\frac{yz}{z+E_2}\right) - d_2 z
\end{aligned} \tag{15}$$

In system (15) the superpredator z predates both x and y. e_1 and e_2 are predation rates of z on x and y respectively, the magnitude of e_1 compared to e_2 determines the preference of z to predate on x compared to y. The parameter c is the efficiency of y and f is the efficiency of z. B, E_1 and E_2 are half saturation constants for the Holling type II predation functions. All other parameters have been defined earlier.

The foraging behaviour of z and its effect on food web dynamics are well studied. Křivan [13] studies the effect of foraging behaviour on the stability of the food web, where e_1 and e_2 are functions of prey and predator population size respectively. If z forages only on the most profitable species, this will destabilise the system. Optimal foraging, i.e. foraging on whatever species is more abundant, stabilises the system and chaos occurs for a smaller range of parameter values. (Křivan [13]).

2.4 Harvesting a species from a food web

Harvesting a species from a 3 species food chain offers insight into the dynamics exhibited by a harvested food chain. Numerical experiments show that

a small increase in harvesting parameter ψ_x can have a catastrophic effect on the food chain. System (16) is a Rosenzweig-Macarthur tritrophic food chain model in which prey species x is harvested at rate ψ_x:

$$\begin{aligned} \dot{x} &= rx\left(1-\frac{x}{K}\right) - b\frac{xy}{x+B} - \psi_x x, \\ \dot{y} &= cb\frac{xy}{x+B} - e\frac{yz}{y+E} - d_1 y, \\ \dot{z} &= f\frac{yz}{z+E} - d_2 z. \end{aligned} \tag{16}$$

All parameters are the same as defined for system (11). In system (16) the harvest yield is proportional to the population of x.

Numerical experiments show if ψ_x =4x10^{-15} all species coexist, while if ψ_x is increased to ψ_x =5x10^{-15} all the species become extinct. This shows that only a tiny amount of the prey population can be harvested in a sustainable manner. It also shows harvesting the species at the bottom of a food chain at a rate higher than is sustainable causes the extinction of all species in the food chain. It is highlights the sensitivity of the harvesting parameter, since a small increase in harvesting can have a big effect on the food web.

The harvesting investigated in this section is when a portion (ψ_x) of the population is removed due to harvesting. Similar analysis can be performed when ψ_x is constant, meaning a constant amount of biomass is removed by harvest no matter what the population is. This method of harvesting is not included as it is of no use in later parts of the paper. Harvesting of the type used in system (16) will be used in the next chapter for harvesting an age-structured population.

Dynamics of harvested populations are very well studied. For example Liu and Chen [14] study a two species competition model, and show that coexistence of two species is possible when one species is periodically harvested. But as the results for system (16) show, the harvesting rate is very sensitive and harvesting at a slightly too high rate leads to extinction.

3 Stage Structured Models

Food web models mentioned in the previous chapter can be useful for studying interacting populations. For more detailed modelling, stage-structure is required. A partial differential equation model can be used to achieve stage-structure in a single population. This can also be achieved using a system of ordinary differential equations as in Cao, Fan and Gard [15] but this method will not be used. The model can structure the population according to length, weight or age. Often length (L) and weight (W) for many species of fish are related by W=dL^b where d and b are weight-length parameters specific to individual species.

3.1 Partial differential equation model

This section investigates the Von Foerster equation, a partial differential equation that models age-structured populations. The Von Foerster equation with an initial condition and boundary value, is from Murray [1]:

$$\frac{\partial n}{\partial a} + \frac{\partial n}{\partial t} = -\mu(a)n, \tag{17}$$

$$n(a,0) = n_0(a), \tag{18}$$

$$n(0,t) = \int_0^\infty \beta(a)n(a,t)da, \tag{19}$$

where $n(a,t)$ is the density of the population of age $a$at time t, and individuals die at rate $\mu(a)$. The death rate μ is a function of age since newborn individuals and very old individuals have higher mortality rates than individuals of other ages.

Equation (18) gives the initial population density of the population. Equation (19) is the renewal condition for the species and determines how many individuals of age zero are produced at time t. Offspring are produced at rate $\beta(a)$, this reproduction rate depends on the age of the individual since individuals of different ages will produce offspring at different rates, e.g. a 10kg red snapper produces 212 times as many eggs as a 1kg snapper (Lubick [18]). Integrating the product of the birth rate and the population density over all ages gives the expected number of offspring. The upper limit of integration in equation (19) is set at ∞ to encompass individuals of all ages. It could be changed to a_{up}, where individuals of age a_{up} or older do not produce offspring

i.e. $\beta(a)$=0 for all $a \geq a_{up}$. The upper limit will be left at ∞ to reduce the need for another parameter.

3.2 Analytic Solution

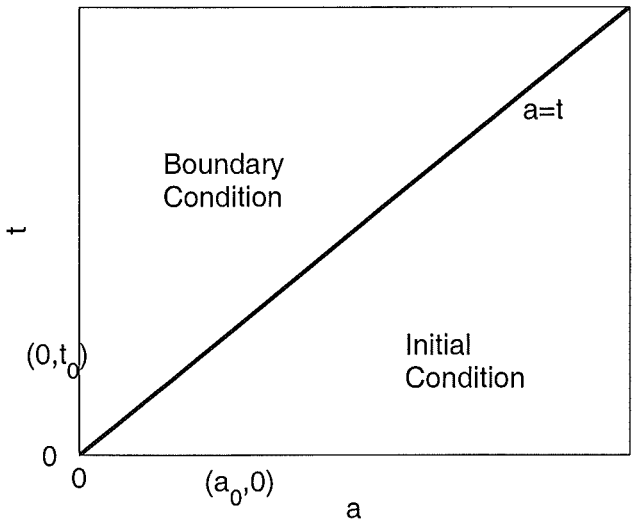

Figure 8: Solution of partial differential equation depends on cases $a > t$ and $a < t$ as shown. If $a > t$ the point $(a_0, 0)$ is used for the initial condition of the characteristic and the initial condition appears in the solution. If $a < t$ the point $(0, t_0)$ is used as the initial condition of the characteristic curve, and the boundary condition appears in the solution in this case.

An analytic solution to the Von Foerster equation (17) with renewal condition (19) is given below, following the approach of Chapman et. al. [16]. The proof uses the method of characteristics in which the partial differential equation is reduced to two ordinary differential equations. In this solution individuals of all ages have the same death rate: $\mu(a) = \mu$ is constant. The birth rate, $\beta(a)$, will remain a function of a.

By the chain rule

$$\frac{dn}{dt} = \frac{dt}{dt}\frac{\partial n}{\partial t} + \frac{da}{dt}\frac{\partial n}{\partial a}, \tag{20}$$

trivially $\frac{dt}{dt} = 1$ and $\frac{da}{dt} = 1$ since species age at the same rate as time passes, i.e. in one unit of time an individual will also age by one unit. The characteristics

are therefore given by $\frac{da}{dt} = 1$. Equation (20) simplifies to $\frac{dn}{dt} = \frac{\partial n}{\partial t} + \frac{\partial n}{\partial a}$, substituting this in equation (17) gives:

$$\frac{dn}{dt} = -\mu n. \tag{21}$$

So along the characteristic curves, $\frac{dn}{dt} = -\mu n$, meaning density decreases at rate μ along the characteristics. The original partial differential equation (17) has now been reduced to two ordinary differential equations.

Solving characteristic $\frac{da}{dt} = 1$ by integrating with respect to t, gives $a = t + c_0$ where c_0 is a constant to be found. Two cases need to be examined, if an individual exists at $t = 0$ i.e. it is a member of the initial population, or if the individual is born at some time $t_0 > 0$. If an individual exists at the start ($t = 0$) then its age is its initial age a_0 plus the time since the model started t. If an individual is born at some time, its age is given by the time since the model started t minus the time at which the individual was born t_0. These two cases give the characteristic curves:

$$a = \begin{cases} t + a_0 & t < a \\ t - t_0 & t > a \end{cases} \tag{22}$$

The form of (22) means there is now two cases to solve for.

3.2.1 Case 1 $a > t$

Integrating (21 gives:

$$\int \frac{dn}{n} = \int -\mu dt.$$

Solving since μ is constant gives:

$$n(a,t) = A_1(a_0)\exp(-\mu t)$$

where $A_1(a_0)$ is a function to be found, depending on a_0. As shown in figure 3.2, for the case $a > t$, the initial condition $(a_0, 0)$ is used for the characteristic curve. The population density $n(a,t)$ must satisfy the initial condition for $t = 0$. Substituting $t = 0$ in the above equation gives:

$$\begin{aligned} n(a_0, 0) = A_1(a_0)\exp(\mu.0) &= n_0(a_0), \\ A_1(a_0) &= n_0(a_0). \end{aligned}$$

From equation (22) the characteristic is given as $a = t + a_0$, so that $a_0 = a - t$, and hence:

$$A_1(a_0) = n_0(a - t). \tag{23}$$

This means the solution is completely defined for the case $a > t$. Now the second case must be examined.

3.2.2 Case 2 $a < t$

Following a similar approach to above, solving (21) gives:

$$n(a, t) = A_2(t_0) \exp(-\mu t),$$

where $A_2(t_0)$ is a function to be found, depending on t_0. In figure 3.2 when $a < t$, the initial condition $(0, t_0)$ is used for the characteristic curve. The characteristic is $a = t - t_0$, substituting $t_0 = t - a$ in the above equation yields:

$$n(a, t) = A_2(t - a) \exp(-\mu t). \tag{24}$$

Since $a < t$, $n(a, t)$ must satisfy the boundary condition (19). Substituting $a = 0$ in the above equation:

$$n(0, t) = A_2(t) \exp(-\mu t) = \int_0^\infty \beta(a) n(a, t) da.$$

The form of $n(a, t)$ is known for two cases, $a > t$ and $a < t$, so separating the above gives:

$$A_2(t) \exp(-\mu t) = \int_0^t \beta(a) n(a, t) da + \int_t^\infty \beta(a) n(a, t) da.$$

The result for $a > t$ is $n(a, t) = n_0(a - t) \exp(-\mu t)$, while for $a < t$, equation (24) gives the form needed. Substituting in the above equation gives:

$$A_2(t) \exp(-\mu t) = \int_0^t \beta(a) A_2(t - a) \exp(-\mu t) da + \int_t^\infty \beta(a) n_0(a - t) \exp(-\mu t) da.$$

Cancelling the common factor of $\exp(-\mu t)$, the above equation simplifies to:

$$A_2(t) = \int_0^t \beta(a) A_2(t - a) da + \int_t^\infty \beta(a) n_0(a - t) da.$$

Define

$$F_1(t) = \int_t^\infty \beta(a) n_0(a-t)da, \tag{25}$$

$$\text{so that} \qquad A_2(t) = \int_0^t \beta(a) A_2(a-t)da + F_1(t).$$

The first term is a convolution by definition. The finite convolution of $\beta(t)$ and $A_2(t)$ is: $\beta(t) \circledast A_2(t) = \int_0^t \beta(a)A_2(a-t)da$ (Farlow [19]). Using this notation, the above equation becomes:

$$A_2(t) = \beta(t) \circledast A_2(t) + F_1(t) \tag{26}$$

To seperate the convolution, Laplace transforms are used, from Farlow [19]: $\mathscr{L}(\beta(t) \circledast A_2(t)) = \mathscr{L}(\beta(t))\mathscr{L}(A_2(t))$, where $\mathscr{L}$ is the Laplace transform with respect to t. Taking the Laplace transform of equation (26) gives:

$$\mathscr{L}(A_2(t)) = \mathscr{L}(\beta(t))\mathscr{L}(A_2(t)) + \mathscr{L}(F_1(t)),$$

$$\mathscr{L}(A_2(t)) = \frac{\mathscr{L}(F_1(t))}{1 - \mathscr{L}(\beta(t))}.$$

Taking inverse laplace transforms to solve for $A_2(t)$:

$$A_2(t) = \mathscr{L}^{-1}\left(\frac{\mathscr{L}(F_1(t))}{1 - \mathscr{L}(\beta(t))}\right). \tag{27}$$

F_1 is given in (25) and $\beta(t)$ is the reproduction rate, now a function of t.The solution for the second case is given in equation (24) where A_2 is defined as in equation (27).

Combining the solution just calculated for $a < t$ with the solution found previously for the case $a > t$ gives:

$$n(a,t) = \begin{cases} n_0(a-t)\exp(-\mu t) & t < a \\ A_2(t-a)\exp(-\mu t) & t > a, \end{cases} \tag{28}$$

where $n_0(a-t)$ is the initial condition given by equation (18) and $A_2(t-a)$ is defined by equation (27). The Laplace transform of $\beta(t)$ in the denominator of (27) means an analytic solution can only be found for simple β, e.g. when it is constant. Most non-trivial choices of β give no analytic solution, as the inverse Laplace transform cannot be found.

An analytic solution of the partial differential equation (17), using equation (28) as the solution with constant birth an mortality rates of $\mu = \frac{1}{5}$, and $\beta = \frac{1}{2}$ respectively, is given in figure 9. A 'top hat' initial condition $n_0 = H(a) - H(a-1)$, where $H(a)$ is the Heaviside function, is used to show convergence of the solution to the typical population structure shown. As figure 9f shows, by t=25, the 'top hat' shape has almost disappeared. The population density for individuals aged 0, starts at $n = 1$ in figure 9a, and grows to $n = 8$ by $t = 25$ in figure 9f. This shows that in a short amount of time the population density has grown large. Using this model, the population will continue to grow unbounded. A more realistic population model would incorporate a bounded population due to competition for resources.

3.3 Steady state population

As shown in Chapman et. al. [16], the model described by equation (17) can be changed to give the population a permanent steady state for all parameter values. Changing (17) to:

$$\frac{\partial n}{\partial t} + \frac{\partial n}{\partial a} = \mu_1 n + \mu_2 N, \tag{29}$$

stops the population from growing unbounded.

In equation (29) $N = \int_0^\infty n(a,t)da$ is the total population size, μ_1 is the natural mortality of the species and μ_2 is mortality due to intraspecific competition.

The model given by equation (29) is very useful for applications since it is unlikely a species will grow unbounded as in figure 9, and it is more likely the population will reach a steady state. The partial differential equation (29) with initial condition (18) and renewal condition (19), will be used in the next chapter to study a specific fish species.

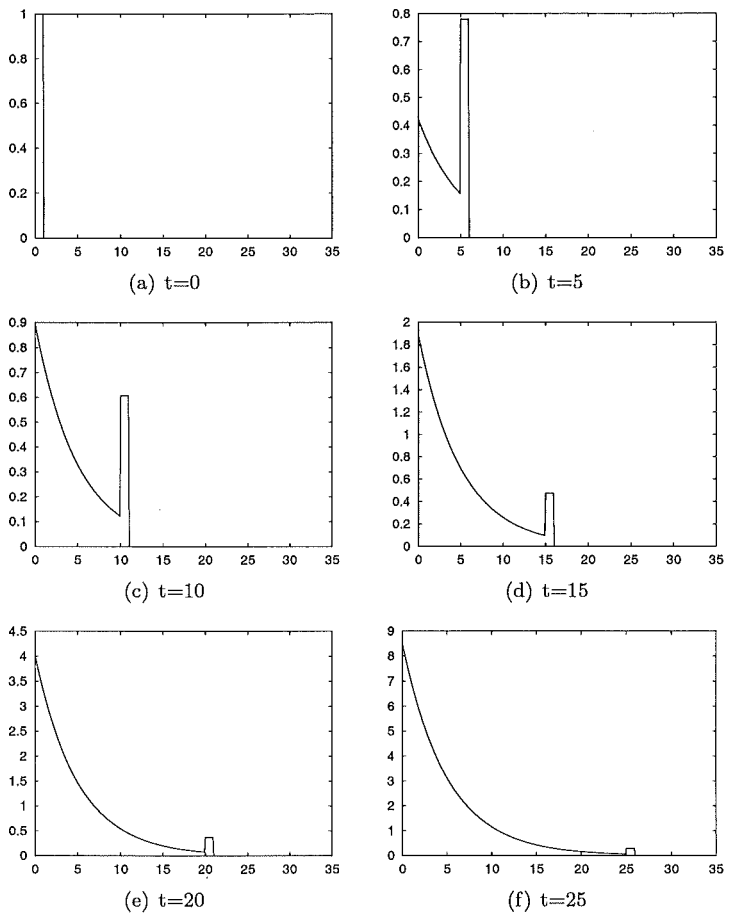

Figure 9: Analytic solution of von Foerster equation (17) with constant reproduction rate $\beta = \frac{1}{2}$ and mortality rate $\mu = \frac{1}{5}$. Each subfigure (a)-(f) shows the population density against age at the time shown in the caption. The 'top hat' initial condition eventually disappears and shows a smooth population structure. Subfigure (f) shows that the population density grows large in only a short time.

3.4 Individual Based Models

Individual based models are very useful for modelling populations. Unlike partial differential equations, they are easy to program and produce results quickly.

The individual model used in this paper, uses the result found when solving the von Foerster equation, $\frac{da}{dt} = 1$. This means all individuals in the model will age at a constant rate of 1, e.g. in one year of time an individual will age one year. Reproduction and mortality rates of individuals are poisson processes with mean rates of $\beta(a)$ and $\mu(a)$ respectively. The use of a poisson process means random events will cause individuals to reproduce or die.

The individual based model described above gives the same results as the Von Foerster equation when the birth rate, mortality rate and initial population are the same. Results from the individual based model are shown against the analytic solution in figure 10, with constant mean birth and death rates of $\beta = \frac{1}{2}$ and $\mu = \frac{1}{5}$ respectively. These are the same values as used for the analytic solution shown in figure 9. The solution for the individual based model has discrete age groups, so is represented by bars, the analytic solution has continuous age groups so is shown by a solid line.

As with the solution for the von Foerster equation given in figure 9, the 'top hat' shape moves along the horizontal axis as time increases, and decays slowly due to mortality. The shape of the population diagrams are exactly the same, both have higher densities for younger populations and the density steadily decreases for older individuals. In each figure, the results from the individual based model are very close to the analytic solution. The small differences between the solutions are due to the small initial population size used for the individual based model.

The next chapter will focus on an application of the individual based model to a real fish population.

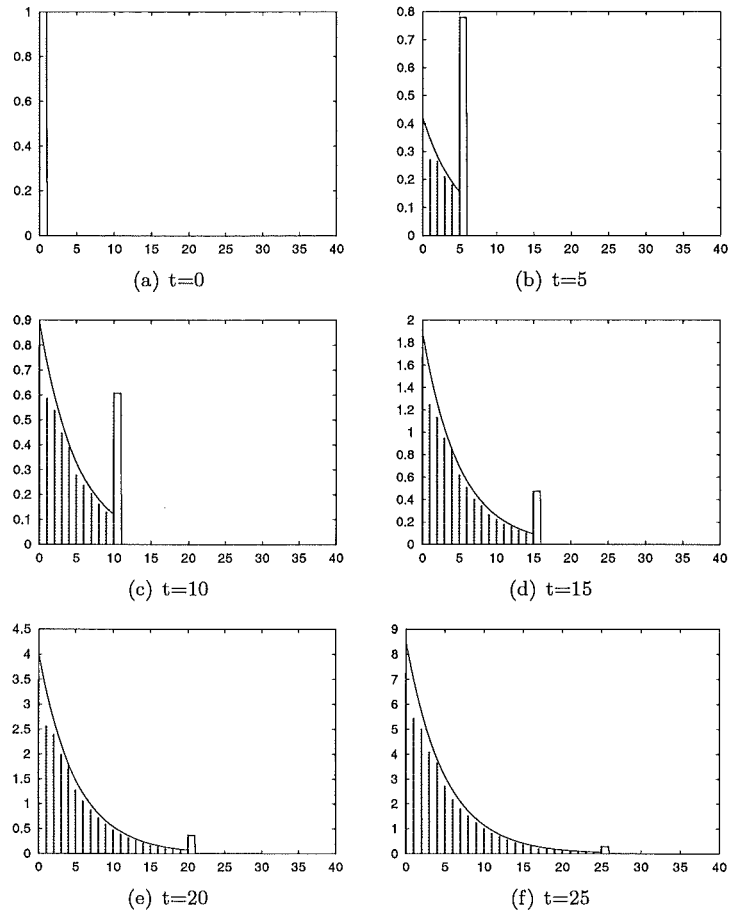

Figure 10: Comparison of population density generated by the individual based model (bars) and the analytic solution (solid line). Each figure shows population density against age at time shown. In the individual based model, all individuals age 1 unit of time for every one unit of time that passes. Reproduction and mortality occur as poisson processes with constant mean rate $\beta = \frac{1}{2}$ and $\mu = \frac{1}{5}$ respectively. The initial population contained 5000 individuals.

4 Case study on orange roughy

In this chapter, a case study of orange roughy (*Hoplostethus atlanticus*) will be examined. An individual based model is used to investigate population dynamics.

Orange roughy stocks in New Zealand waters are currently depleted and still being fished. Harvesting rates of orange roughy are examined in detail in this chapter, particularly to see if any harvesting rate is sustainable. The effect of different parameter values on population biomass is studied, especially since many parameters such as natural mortality, maturity age and stock-recruitment steepness are only educated guesses.

4.1 Background

Orange roughy are a deepwater fish, living at depths of 700-1500m, well below the continental shelf where most fisheries exist (Clark [20]). There are orange roughy fisheries off the coast of New Zealand, Australia and Namibia (Clark, Anderson, Francis and Tracey [26]). Orange roughy diet consists mostly of squid and other fish when older, and molluscs at a young age (Bulman and Koslow [21]).

The deepwater environment is very arid and unable to support fast growing species. Orange roughy are a slow growing fish, have high maturity age and low recruitment. This makes them highly susceptible to overfishing (Clark [20]). The ORH3B Northwest Chatham rise fishery is located within New Zealand's exclusive fishing zone, off the east coast of the South Island. Statistics from this fishery are used, as they are indicative of all orange roughy fisheries in New Zealand.

The orange roughy fishery started in 1978-79 with catch rates between 15,400t and 32,800t throughout the 1980's. Table 1 shows the Chatham rise fishery peaked in the 1988-89 fishing year with total allowable catch (TAC) of 38,300 tonnes and recorded catch of 32,785 tonnes. Table 1 shows TAC was reduced to 12,700 tonnes in 1995-6, and has remained constant at this rate. Reported catch size also decreased to a minimum of 8,663t in 1999-2000, but has since increased slightly to 12,333t in 2002-3.

From Francis [25], the virgin biomass (B_0) of the Chatham Rise has a best estimate of 401,000 tonnes, but was reduced by 80% to 82,00t in 1997 (Clark

Fishing Year	Reported Catch (t)	Total Allowable Catch (t)
1979-80	11800	–
1980-81	31100	–
1981-82	28200	23000
1982-83	32605	23000
1983-84	32535	30000
1984-85	29340	30000
1985-86	30075	29865
1986-87	30689	38065
1987-88	24214	38065
1988-89	32785	38300
1989-90	31669	32787
1990-91	21521	23787
1991-92	23269	23787
1992-93	20048	21300
1993-94	16960	21300
1994-95	11891	14000
1995-96	12501	12700
1996-97	9278	12700
1997-98	9638	12700
1998-99	9372	12700
1999-2000	8663	12700
2000-01	9274	12700
2001-02	11325	12700
2002-03	12333	12700

Table 1: Catch data for Chatham Rise orange roughy fishery (ORH3B), from [27]. There was no TAC set for years 1979-81.

et. al. [26]). The best estimate of maximum sustainable yield is 2.7% of virgin biomass, the maximum constant yield is thought to be 2/3 x maximum sustainable yield = 1.8% of B_0 (Francis [25]). With estimated biomass of 82,000t in 1997, using the reported catch for 1997-8 from table 1, the harvest rate in 1997 wass $\frac{9638}{82000} = 0.1175$ which is approximately equal to 12% of that years biomass. This harvest rate is also equal to 2.5% of the virgin biomass. Although this harvest rate is just above the maximum sustainable yield of 1.8% with respect to virgin biomass, the harvest rate of 12% of current biomass is alarmingly high. Section 4.3 shows this harvesting rate is not sustainable, and investigates more realistic harvest rates.

Parameter	Symbol	Value
Stock Recruitment Steepness	h	0.95
External mortality	μ_1	$0.03yr^{-1}$
Internal mortality	μ_2	$0.03yr^{-1}$
Growth Parameters:	L_∞	42.5cm
	k	$0.059yr^{-1}$
	t_0	-0.346yr
Weight-Length Parameters	d	0.0963
	b	2.68
Maturity Age	a_m	23years
Fishable age	a_f	23years
Virgin Biomass (1978 estimate)	B_0	411000tonnes
Virgin Adult Biomass (1978 estimate)	A_0	300000tonnes
Initial Recruitment	R_0	0.3

Table 2: Parameter values for Orange Roughy used in the individual based model. The value for R_0 is an educated guess, all other parameters are from [25] and [26].

4.2 The Model

The individual based model used has reproduction rate β generated by the Beverton-Holt stock recruitment model, and mortality rate $\mu = \mu_1 + \mu_2 N$ as defined for equation (29). This mortality rate is used as the solution to equation (29) has a steady state population for all parameter values, so the individual based model will also have this steady state population. This mortality is used as orange roughy populations have not grown unbounded.

The Beverton-Holt stock recruitment model determines recruitment rate in a given year according to the biomass of mature fish in the previous year. The form of Beverton-Holt recruitment is (Francis [25]):

$$R_i = \frac{A_{i-1}}{\alpha + \gamma A_{i-1}}, \quad i = 1, 2 \ldots, \tag{30}$$

where R_i and B_i are recruitment rate and biomass of fish at time $t = i$ respectively. Parameters α and γ have no simple biological interpretation, and are

calculated by ([25]):

$$\alpha = \frac{A_0(1-h)}{4hR_0},$$
$$\gamma = \frac{(5h-1)}{4hR_0},$$

where h is the stock-recruitment steepness, A_0 is the biomass of mature fish in the initial population and R_0 is the virgin recruitment rate, i.e. rate of recruitment at the start of the model, and can be estimated or calculated. The value of R_0 is not important for the Beverton-Holt recruitment model, and changing its value has little affect on population dynamics. An educated guess of $R_0 = 0.3$ as given in table 2, is used.

In the model, mature fish of age a_m or older reproduce, since only mature orange roughy are capable of producing offspring. The probability of a mature individual giving birth to one offspring that enters the model, i.e. reaches 1 year of age, is equal to the recruitment rate divided by the number of mature individuals:

$$\beta_i = \frac{R_i}{M_i}, \quad i = 0, 1, 2 \ldots,$$

where R_i is the recruitment rate given in the Beverton-Holt recruitment model (30), and M_i is the number of mature fish alive at any time.

The length L (in cm) of a fish is calculated by the deterministic von Bertalanffy growth formula from Francis [25]:

$$L = L_\infty(1 - \exp(-k(a_j - t_0))).$$

Where L_∞ is the maximum length (cm) an individual can reach, k is the von Bertalanffy growth rate and t_0 is a constant (all values given in table 2). a_j is the age (in years) of individual j.

The mass in grams (W) of an individual is calculated by $W = dL^b$ where L is the length in cm, and d and b are weight-length conversion parameters ([25]), specified in table 2. The biomass of the population is calculated as the combined mass of all individuals alive.

On average mature female orange roughy produce between 26000 and 49000 eggs per kg of body weight (Clark et al. [24]). Very few of these eggs reach 1 year of age, so the model used only includes individuals of age 1 year or older.

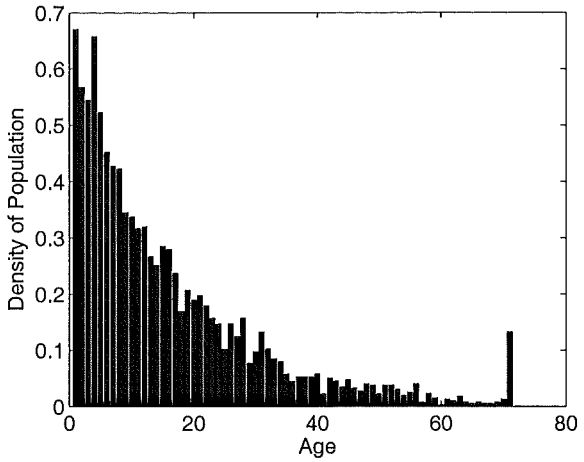

Figure 11: Population density of orange roughy against age at steady state. Parameter values are listed in table 2. The spike in population density at age 70 is due to all orange roughy of age 70 and over being included in this group. Orange roughy are long lived and can live up to 150 years of age.

Using the parameters in table 2 the individual based model gives figure 11 as the steady state population. The figure shows population density for fish of different ages. The spike in figure 11 for fish of age 70 encompasses all fish of age 70 or older. This density is high as orange roughy are long lived (Clark [20]) and can live up to 150 years. The figure shows a typical population structure - larger densities of young fish and decreasing densities of older fish, due to mortality. The relatively large density of older fish is because orange roughy are long lived and have low natural mortality.

4.3 Can orange roughy be harvested sustainably?

The model used only removes orange roughy due to harvesting at a constant rate. It does not take into account environmental damage, by catch of other species, catching underage fish or preferential targeting of large fish. These assumptions are unrealistic since orange roughy are caught by bottom trawling which causes significant environmental damage and the fishery also has significant bycatch (Reference here).

Figure 12 shows the structure of an orange roughy population that has been

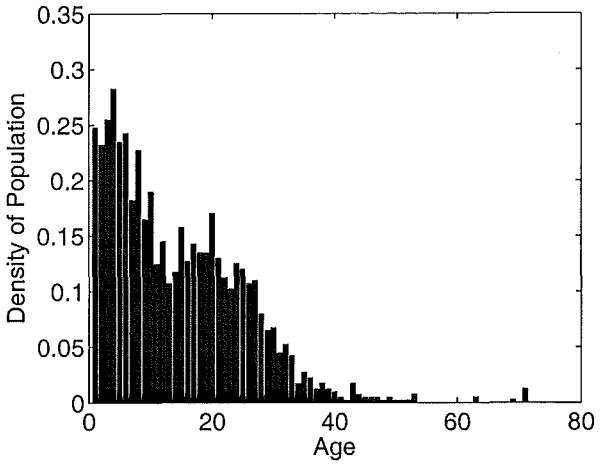

Figure 12: Structure of orange roughy population that has been harvested at a constant rate of 10% of the population per year for 25 years. Only fish 23 years of age and older over are harvested. The harvesting has had a very big affect on the population, densities of old fish are very low, with many age groups having zero density. All parameters listed in table 2.

harvested for 25 years. All parameter values are given in table 2 and are exactly the same as parameters used for figure 11. The only difference is that fish of age a_f and over in the population shown in figure 12 have been harvested at a constant rate with 10% of the fishable population removed by harvesting each year. Figure 12 shows a big decrease in population density of fish of all ages, when compared to figure 11. The harvesting causes a big decrease in population density of young fish, figure 12 shows the density of fish aged between 1 and 5 is around 0.25, whereas in figure 11 densities are 0.5 or higher for the same age group. The decrease in immature fish is due to decreased recruitment because of a smaller mature population.

Harvesting has also had a large affect on mature fish, there are a lot of gaps in figure 12, that show that the density for some age groups is zero as all fish of that age have been removed by harvesting. The large spike present in figure 11 for orange roughy of age 70 and older has been significantly decreased by the harvesting. For the unfished population, this density is 0.15, but after harvesting the density has decreased to 0.02.

Figure 13 plots the percentage of virgin biomass present against harvest rate,

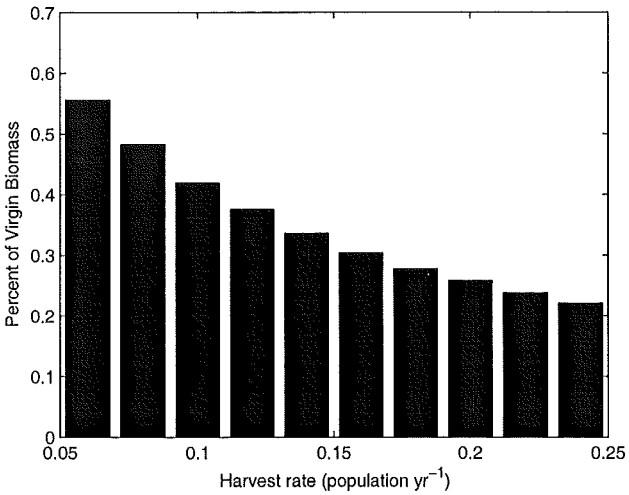

Figure 13: Affect of different harvest rates on biomass of orange roughy population. Shows the percent of virgin biomass present after 25 years of constant harvesting at a given rate. All parameters used are given in table 2.

to show the decrease in biomass caused by harvesting. Figure 13 shows that all harvest rates tested caused a significant drop in population biomass. The results were generated by allowing the model to run for long enough for the population to reach steady state (t=75 was used for this), then the population was harvested for 25 years, since this is approximately the length of time the orange roughy fishery has existed. The lowest harvest rate tested 0.06popnyr^{-1} caused a 45% decrease in population biomass, and the highest value of 0.24popnyr^{-1} decreased biomass to just 22% of the original biomass. Clark et. al. [26] estimate an 80% decrease in orange roughy biomass, figure 13 shows a harvest rate of 0.24 for 25 years nearly causes this much of a decrease.

Orange roughy in the Chatham rise fishery continue to be fished, even though their population is at a very low level. Using the individual based model developed, harvest rates are examined to see if continual harvesting is sustainable for the survival of this population.

Table 3 gives projected biomass of orange roughy in the Chatham Rise fishery in 25 years time (2030) and in 50 years (2055) for different rates of harvesting. The figures for projected biomass are based on a 2005 biomass of 82,000 tonnes, the same as estimated 1997 biomass (Clark et. al. [26]). It is unlikely the 2005

Harvesting Rate (popnyr^{-1})	**Projected 2030 Biomass** (,000 tonnes)	**Projected 2055 Biomass** (,000 tonnes)	**Trend**
0	97	96	$\uparrow$
0.01	88	78	$\rightarrow$
0.02	80	66	$\downarrow$
0.03	71	51	$\downarrow$
0.04	64	43	$\downarrow$
0.05	60	38	$\downarrow$
0.06	55	31	$\downarrow$
0.07	51	27	$\downarrow$
0.08	47	23	$\downarrow$
0.09	44	21	$\downarrow$
0.10	41	18	$\downarrow$

Table 3: Orange roughy population biomass response to different harvesting rates. Shows harvesting rate, biomass in 2030 and 2055 and the trend shown. 2005 biomass is estimated at 82,000 tonnes. Results were generated by an individual based model using parameters given in table 2. Current harvest rates are estimated at 0.12 popnyr^{-1}, the results show harvest rates this high are not sustainable.

biomass is the same as 1997 biomass, but no more recent biomass estimates are available.

As shown in table 3 the only harvesting rate that leads to a long term increase in biomass is zero. A harvesting rate of 0.01 causes the projected biomass to increase in 25 years, but decrease slightly in 50 years. Given that in the last 26 years the biomass has decreased by over 300,000 tonnes, the decrease of 4,000 tonnes in 50 years is very small and this harvest rate is considered sustainable. All higher harvesting rates lead to a decrease in medium term biomass and an even bigger decrease in long term biomass. Francis [25] gives a maximum sustainable harvesting rate as 0.018 of the population per year, this harvest rate was not tested, but a similar harvest rate (0.02) caused a decrease in long term biomass. This harvest rate is sustainable in the short term, but by 2055 is significantly lower at 66,000 tonnes. The highest harvesting rate tested, 0.1 of the population per year, leads to a very big decrease in biomass, with projected 2055 biomass of just 18,000 tonnes.

The results in table 3 show a maximum sustainable harvest rate of 0.01 of the population per year. Based on current biomass of 82,000 tonnes, this gives

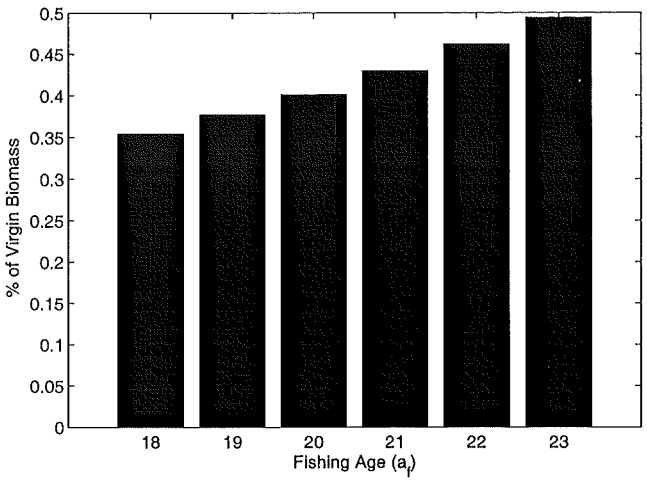

Figure 14: Affect of fishing age on biomass of orange roughy population. Shows fishing age (years) against percent of virgin biomass. The population of fish aged a_f and over is harvested at a constant rate of 0.1 popnyr^{-1} for 25 years. Results generated for maturity age held constant at 23 years. If a_f is less than 23 this means immature orange roughy are fished.

a maximum sustainable yield of 820 tonnes per year. As shown in table 1 the total allowable catch for the year 2002-2003 was 12,700 tonnes or over 15 times as high as the sustainable harvest yield generated by the model. As already stated, this equates to a harvest rate of 0.12 of the population per year. This is higher than the maximum harvest rate tested in the model. The harvest rate of 0.1 of the population per year is shown to be unsustainable, this also shows the current rate of harvesting is unsustainable.

4.4 Parameter sensitivity

Figure 14 shows that biomass is affected by the fishing age a_f. Results for this figure were generated with maturity age held fixed at $a_m = 23$ years, while the fishable age varied. The figure shows decreasing the fishing age results in a decrease in biomass. This is not surprising since harvesting immature fish will result in lower recruitment as fish are removed before they have the opportunity to reproduce.

Stock-recruitment steepness (h) had little affect on the biomass of the pop-

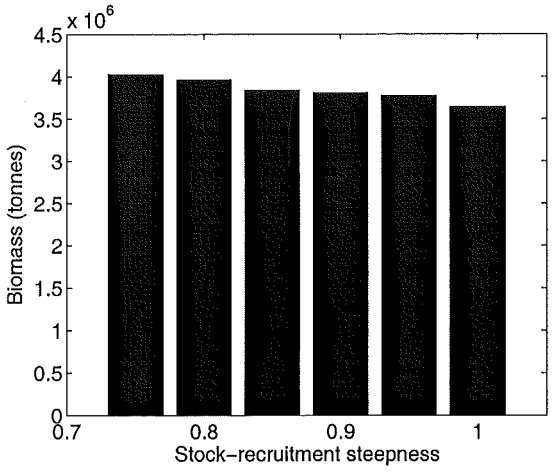

Figure 15: Effect of stock-recruitment steepness on biomass of population. Values tested are less than 1 as this is the maximum value expected for stock-recruitment steepness Francis [25].

ulation. The value of $h = 0.95$ in table 2 is an educated guess in Francis [25]. The results in figure 15 show changing the value of h has little effect on biomass. Increasing h causes a small decrease in biomass, but it is relatively small. Values for stock-recruitment steepness tested are less than 1 as it is unlikely to be higher (Francis [25]).

Increasing mortality rates decreased population biomass as shown in figure 16. This is trivial, if fish die at a faster rate then the population will have fewer fish and hence will have lower biomass, while decreasing the mortality rate increases biomass. Figure 16 shows changes in natural mortality rate cause significant changes in biomass. The value of this parameter is very important as differences in its value can cause big changes in biomass.

4.5 Further Research

It is unlikely that orange roughy recruitment is related to the biomass of the population by a deterministic formula, such as the Beverton-Holt stock recruitment model used. It is more likely that recruitment varies yearly, as a stochastic process. The effect of harvesting an orange roughy population with stochastic recruitment should be investigated. The model could be made more realistic by including a parameter that measures environmental damage, be-

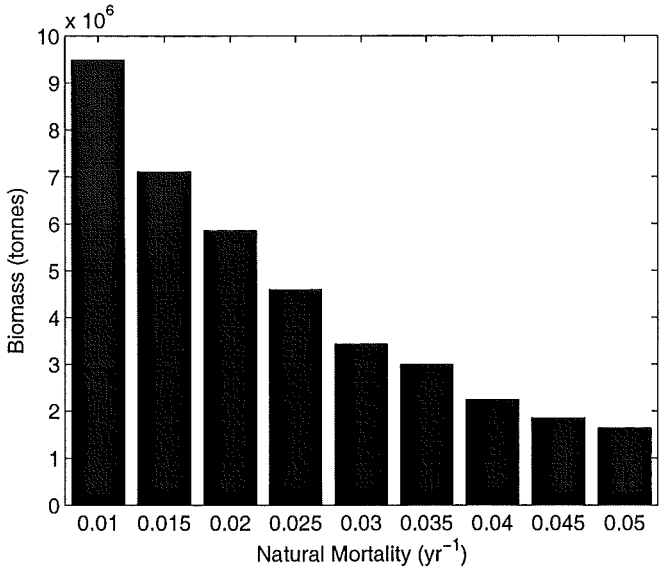

Figure 16: Effect of natural mortality μ_1 on biomass of population. 0.03 is the most likely value, but values tested are small as orange roughy have low natural mortality Clark [20].

cause environmental damage could increase mortality and hence the population biomass.

5 Conclusion

Chapter 1 dealt with simple deterministic food web models with two species. These are easy to analyse and offer some applications in the form of phytoplankton/zooplankton modelling. They exhibit relatively simple behaviour and have a stable fixed point or a stable limit cycle. Predator-prey, mutualisms and competition behaviour can all be modelled using food web models with two species.

Chapter 2 showed that the inclusion of one more species makes the analysis of food webs much harder, and also changes the complexity that a system can exhibit. With three species, the system could exhibit chaos as well as fixed points and limit cycles. Different topologies of food webs have different dynamics, only some topologies produce chaos. A three species food web also offered more realistic modelling of two species competing for the same resource, and showed that under certain situations competing predators could coexist. Harvesting a species at a constant rate can also be included in a three species food web model. For some harvesting parameter values the population dynamics are unchanged, but increasing the harvesting rate above the critical value can kill off the harvested species.

The deterministic models in chapter 1 and 2 can be useful for modelling interacting populations. The partial differential equation models considered in chapter 3 can model a single species with stage structure. Chapter 3 showed a partial differential equation with a renewal condition that governs birth of individuals, and initial population density can be used to model a population with age-structure. Analytic solutions of partial differential equations are difficult to obtain, the von Foerster equation used in chapter 3 only only gives an analytic solution for a trivial renewal condition. The von Foerster equation can be approximated by an individual based model, and the solutions of the individual based model and partial differential equation are very similar for a trivial renewal condition, even when a small initial population is used.

In chapter 4 an individual based model was used to look at orange roughy in the Chatham rise fishery. Higher values of natural mortality gives a lower biomass, harvesting fish before they reach maturity was also shown to decrease population biomass. The affect of harvesting the fishery at a constant rate was examined. Results from the individual based model show that higher harvest rates give lower biomass of the population. Investigating the continual harvesting of the population to predict future population biomass, gave a sustainable harvesting rate. The model used in chapter 4 gave a sustainable catch rate

of 820 tonnes per year. Total allowable catch rates for orange roughy in the Chatham rise fishery are currently 12,700 tonnes per year, or over 15 times the sustainable rate calculated from the model.

A Appendix

The linearisation (Jacobian) matrix of a dynamical system of the form:

$$\dot{x} = f(x, y),$$
$$\dot{y} = g(x, y),$$

is given by:

$$A = \begin{bmatrix} \frac{\partial f}{\partial x} & \frac{\partial f}{\partial y} \\ \frac{\partial g}{\partial x} & \frac{\partial g}{\partial y} \end{bmatrix}. \tag{31}$$

Therefore the Jacobian of the Lotka-Volterra system (2) is given by:

$$A = \begin{bmatrix} a - by & -bx \\ cy & cx - d \end{bmatrix}, \tag{32}$$

Substituting in fixed point (0,0) gives the matrix:

$$A = \begin{bmatrix} a & 0 \\ 0 & -d \end{bmatrix}.$$

Giving $\det(A)=-ad$, and $\text{trace}(A)=a-d$. Substituting in the second fixed point $(\frac{d}{c}, \frac{a}{b})$ gives:

$$A = \begin{bmatrix} 0 & -\frac{bd}{c} \\ \frac{ac}{b} & 0 \end{bmatrix},$$

giving $\det(A)=ad$ and $\text{trace}(A)=0$.

Also since the Lotka-Volterra system is so simple, $\frac{dy}{dx}$ is seperable, and hence there is a conserved quantity in this system. By the chain rule:

$$\frac{dy}{dx} = \frac{dy}{dt}\frac{dt}{dx} = \frac{\dot{y}}{\dot{x}},$$

substituting in for $\dot{x}$, $\dot{y}$:

$$\frac{dy}{dx} = \frac{(cx - d)y}{(a - by)x},$$

seperating and integrating to solve:

$$\int \frac{a-by}{y} dy = \int \frac{cx-d}{x} dx$$
$$a\log(y) - by = cx - d\log(x) + K,$$

where K is a constant of integration. Hence the conserved quantity $V(x,y)$ is given by:

$$V(x,y) = a\log(y) + d\log(x) - by - cx.$$

B Appendix

The predator prey food web with Holling type II predation functions described by system (6) is:

$$\dot{x} = rx\left(1 - \frac{x}{K}\right) - A\frac{xy}{x+B}$$
$$\dot{y} = c\frac{xy}{x+B} - dy$$

x is prey, y is predator and t is time. Introduce new dimensionless variables: prey N, predator P, and time τ:

$$x = BN,\ y = r\frac{B}{A}P,\ \tau = rt. \tag{33}$$

A check is done at the end of the appendix to show N, P and τ are all dimension free. Changing to dimensionless prey N, by the chain rule:

$$\begin{aligned}
\dot{N} = \frac{dN}{d\tau} &= \frac{dN}{dx}\frac{dx}{dt}\frac{dt}{d\tau} \\
&= \frac{1}{B}\frac{1}{r}\left(rx(1-\frac{x}{K}) - A\frac{xy}{x+B}\right) \\
&= \frac{1}{B}\frac{1}{r}\left(rBN(1-\frac{BN}{K}) - A\frac{BNr\frac{B}{A}P}{BN+B}\right) \\
&= N(1-\frac{BN}{K}) - \frac{B^2NrP}{rB^2(N+1)} \\
&= N(1-\frac{BN}{K}) - \frac{NP}{N+1} \\
&= N(1-\frac{N}{\rho}) - \frac{NP}{N+1},
\end{aligned}$$

where $\rho = \frac{K}{B}$.

Now for P

$$\begin{aligned}
\dot{P} = \frac{dP}{d\tau} &= \frac{dP}{dy}\frac{dy}{dt}\frac{dt}{d\tau} \\
&= \frac{A}{Br}\frac{1}{r}\left(\frac{cxy}{x+B} - dy\right) \\
&= \frac{A}{Br^2}\left(\frac{cBN\frac{rB}{A}P}{BN+B} - d\frac{rB}{A}P\right) \\
&= \frac{cB^2rNP}{B^2r^2(N+1)} - \frac{drAB}{ABr^2}P \\
&= \frac{cNP}{r(N+1)} - \frac{d}{r}P \\
&= \frac{c}{r}\left(\frac{N}{N+1} - \frac{d}{c}\right)P \\
&= \beta\left(\frac{N}{N+1} - \alpha\right)P,
\end{aligned}$$

where $\beta = \frac{c}{r}$ and $\alpha = \frac{d}{c}$.

Checking to ensure all new parameters are in fact dimensionless. Original parameters have dimensions: x=prey, y=predator, t=time, $r = \frac{1}{\text{time}}$, K=prey, $A = \frac{\text{prey}}{\text{predator time}}$, B=prey, $c = \frac{1}{\text{time}}$, $d = \frac{1}{\text{time}}$.

$$\begin{aligned}
N &= \frac{x}{B} = \frac{\text{prey}}{\text{prey}} = 1 \\
P &= \frac{Ay}{rB} = \frac{\frac{\text{prey}}{\text{predator time}}\text{predator}}{\frac{1}{\text{time}}\text{prey}} = \frac{\frac{\text{prey}}{\text{time}}}{\frac{\text{prey}}{\text{time}}} = 1 \\
\tau &= rt = \frac{1}{\text{time}}\text{time} = 1 \\
\rho &= \frac{K}{B} = \frac{\text{prey}}{\text{prey}} = 1 \\
\beta &= \frac{c}{r} = \frac{\frac{1}{\text{time}}}{\frac{1}{\text{time}}} = 1 \\
\alpha &= \frac{d}{c} = \frac{\frac{1}{\text{time}}}{\frac{1}{\text{time}}} = 1.
\end{aligned}$$

So all parameters are dimensionless.

C Appendix

The Jacobian of the non-dimensionalised two species food web described by system (7), is:

$$A = \begin{bmatrix} 1 - \frac{2N}{P} - \frac{P}{N+1} + \frac{NP}{(N+1)^2} & -\frac{N}{N+1} \\ \frac{\beta P}{(N+1)^2} & \beta\left(\frac{N}{N+1} - \alpha\right) \end{bmatrix}. \tag{34}$$

Solving $\dot{N} = \dot{P} = 0$ in (7) gives three fixed points: (0,0), (ρ,0) and $\left(-\frac{\alpha}{\alpha-1}, -\frac{\alpha+\alpha\rho-\rho}{\rho(1-2\alpha+\alpha^2)}\right)$. Substituting (0,0) in the jacobian matrix (34) gives:

$$A = \begin{bmatrix} 1 & 0 \\ 0 & -\alpha\beta \end{bmatrix}, \tag{35}$$

which has eigenvalues 1,-$\alpha\beta$, which are real for all α, β real. Hence limit cycles will not occur at (0,0).
Substituting (ρ,0) in (34) gives:

$$A = \begin{bmatrix} 1 & \frac{-\rho}{\rho+1} \\ 0 & -\frac{\beta(\alpha+\alpha\rho-\rho)}{\rho+1} \end{bmatrix}, \tag{36}$$

which has eigenvalues 1, $-\frac{\beta(\alpha+\alpha\rho-\rho)}{\rho+1}$, which are real for all α, β, ρ real, hence will not have a limit cycle for any parameter values. Substituting the third fixed point $\left(-\frac{\alpha}{\alpha-1}, -\frac{\alpha+\alpha\rho-\rho}{\rho(1-2\alpha+\alpha^2)}\right)$ in (34):

$$A = \begin{bmatrix} \frac{\alpha(\rho\alpha+\alpha+1-\rho)}{\rho(\alpha-1)} & -\alpha \\ -\frac{\beta(\alpha+\alpha\rho-\rho)}{\rho} & 0 \end{bmatrix}. \tag{37}$$

The eigenvalues of (37) are complex for most choices of α, ρ, β. The real part of the eigenvalues is $\frac{\alpha^2+\alpha-\alpha\rho+\rho\alpha^2}{\rho(2\alpha-2)}$. Limit cycles occur when the real part of the eigenvalues is zero, solving $\frac{\alpha^2+\alpha-\alpha\rho+\rho\alpha^2}{\rho(2\alpha-2)} = 0$, gives $\rho = \frac{1+\alpha}{1-\alpha}$. Numerical results show for $\rho < \frac{1+\alpha}{1-\alpha}$, the fixed point $\left(-\frac{\alpha}{\alpha-1}, -\frac{\alpha+\alpha\rho-\rho}{\rho(1-2\alpha+\alpha^2)}\right)$ is a stable fixed point, while for $\rho > \frac{1+\alpha}{1-\alpha}$, a stable limit occurs around the fixed point.

References

[1] MURRAY J. D., *Mathematical Biology*, Springer-Verlag, New York, 1989.

[2] KOT M., *Elements of Mathematical Ecology*, University Press, Cambridge, 2001.

[3] GILPIN M.E., *Do hares eat lynx?*, The American Naturalist, The University of Chicago Press, 107(1973), pp. 727–730.

[4] MAY R. M., *Mathematical aspects of the dynamics of animal populations*, in *Studies in Mathematical Biology Part II: Populations and communities*, S. A. LEVIN (ed.), The Mathematical Association of America, 1978.

[5] BOYCE W. E. AND R. C. DIPRIMA, *Elementary Differential equations and boundary value problems 7th Ed.*, John Wiley & Sons Inc., New York, 2001.

[6] TRUSCOTT J. E. AND J. BRINDLEY, *Ocean Plankton Populations as Excitable Media*, Bulletin of Mathematical Biology, Pergamon-Elsevier Science LTD., 56 (1994), pp. 981–998.

[7] WALTMAN P., *Competition Models in Population Biology*, Society for Industrial and Applied Mathematics, Pennsylvania, 1983.

[8] HSU S. B., S. P. HUBBELL AND P. WALTMAN, *A Contribution to the Theory of Competing Predators*, Ecological Monographs, The Ecological Society of America, 48 (1978), pp. 337–349.

[9] DE FEO O. AND S. RINALDI, *Yield and Dynamics of Tritrophic Food Chains*, The American Naturalist, The University of Chicago Press, 150 (1997), pp. 328–345.

[10] HASTINGS A. AND T. POWELL, *Chaos in a Three-Species Food Chain*, Ecology, The Ecological Society of America, 72 (1991), pp. 896–903.

[11] CAMPBELL N. A., J. B. REECE AND L. G. MITCHELL, *Biology 5th edition*, Benjamin Cummings, Merlo Park California, 1997.

[12] MURPHY D. J. AND D. KELLY, *Seasonal variation in the honeydew, invertebrate, fruit and nectar resource for bellbirds in a New Zealand mountain beech forest*, New Zealand Journal of Ecology, New Zealand Ecological Society, 27 (2003), pp. 11–24.

[13] KŘIVAN V., OPTIMAL FORAGING AND PREDATOR-PREY DYNAMICS, Theoretical Population Biology, Elsevier Inc., 49 (1996), pp. 265–290.

[14] LIU B. AND L. CHEN, *The periodic competing Lotka-Volterra model with impulsive harvest*, Mathematical Medicine and Biology, Institute of Mathematics and its Applications, 21 (2004), pp. 129–145.

[15] CAO Y., J. FAN AND T. C. GARD, *The effects of state-dependent time delay on a stage-structured population growth model*, Nonlinear Analysis, Theory, Methods & Applications, Pergamon Press Ltd., 19 (2002), pp. 95–105.

[16] CHAPMAN S. J., M. PLANK AND A. JAMES, *A nonlinear model of size-structured populations with applications to cell cycles*, submitted, 2005.

[17] NORHAYATI AND G. C. WAKE, *The solution and the stability of a nonlinear age-structured population model*, ANZIAM Journal, Australian Mathematical Society, 45 (2003), pp. 153–165.

[18] LUBICK N., *A team effort benefits fishery and community*, Marituentas, The Pew Fellows program in marine conservation, 4 (2003), pp. 22–26.

[19] FARLOW S.J., *Partial differential equations for scientists and engineers*, John Wiley & Sons, New York, 1982.

[20] CLARK M. R., *Are deepwater fisheries sustainable? - the example of orange roughy (Hoplostethus atlanticus) in New Zealand*, Fisheries Research, Elsevier Science B.V., 51 (2001), pp. 123–135.

[21] BULMAN C. M. AMD J. A. KOSLOW, *Diet and food-consumption of a deep-sea fish, orange roughy hoplostethus-atlanticus (Pisces, Trachichthyidae), off southeastern Australia.*, Marine Ecology-Progress series, Inter-Research, 82 (1992), pp. 115–129.

[22] FRANCIS R. I. C. C., D. C. SMITH, *Mean length, age, and otolith weight as potential indicators of biomass depletion for orange roughy, Hoplostethus atlanticus*, New Zealand Journal of Marine and Freshwater Research, The Royal Society of New Zealand, 29 (1995), pp. 581–587.

[23] CATCH DATA FOR ORANGE ROUGHY FISHERIES IN NEW ZEALAND, *From: http://www.fish.govt.nz/sustainability/research/planning/medium/deepwater6.htm#orgnor*, 1.23pm Thursday 4th August.

[24] CLARK M. R., D. J. FINCHAM AND D. M. TRACEY, *Fecundity of orange roughy (Hoplostethus atlanticus) in New Zealand waters*, New Zealand Journal of Marine and Freshwater Research, The Royal Society of New Zealand, 28 (1994), pp. 193–200.

[25] FRANCIS R. I. C. C., *Use of risk analysis to assess fishery management strategies: a case study using orange roughy (Hoplostethus atlanticus) on the Chatham rise, New Zealand*, Canadian Journal of Fisheries and Aquatic Sciences, National Researh Council Canada, 49 (1992), pp. 922–930.

[26] CLARK M. R., ANDERSON O. F., FRANCIS R.I.C.C. AND TRACEY D. M., *The effects of commercial exploitation on orange roughy (Hoplostethus atlanticus) from the continental slope of the Chatham rise, New Zealand, from 1979 to 1997* , Fisheries Research, Elsevier Science B.V., 45 (2000), pp. 217–238.

[27] CATCH DATA AND TAC FOR ORH3B FISHERY, *From: http://www.fish.govt.nz/sustainability/research/assessment/plenary/orh3B.pdf* Friday 9 September 1.14pm.